PHYSICAL REVIEW B **89**, 121416(R) (2014)

Minimum-scattering superabsorbers

Nasim Mohammadi Estakhri and Andrea Alù
Department of Electrical and Computer Engineering, The University of Texas at Austin, Austin, Texas 78712, USA
(Received 19 October 2013; revised manuscript received 2 March 2014; published 31 March 2014)

Absorption and scattering are inherently related, as it is not possible to absorb power without creating a far-field shadow. We show, however, that properly overlapped resonant modes in a suitably designed system may in principle lead to arbitrarily large absorption levels, while at the same time minimizing the total scattering. We discuss the fundamental limits on scattering and absorption of an arbitrary receiving system and envision a composite nanoparticle that demonstrates the concept of a minimum-scattering superabsorber, with potential applications in energy harvesting, sensing, and imaging.

DOI: 10.1103/PhysRevB.89.121416 PACS number(s): 42.25.Bs, 07.07.Df, 42.50.Gy, 42.68.Mj

Scattering from sensors and receivers is in general unavoidable, but at the same time it is often undesired, especially in near-field subdiffractive imaging [1,2] or for closely spaced receivers and energy harvesters, due to unwanted perturbations on the incoming wave. To address this problem, optimal designs for "minimum-scattering" receiving antennas and sensors have been extensively discussed at radio frequencies [3–6], yet typically producing largely suboptimal absorption levels. A sensor or an absorber designed to maximize the amount of received power is typically required to operate under a conjugate-matched condition [7–9], also known in optics as coherent perfect absorption [10], but this comes at the price of scattering an equal amount of power as it receives, significantly perturbing the impinging wave [11,12]. It is reasonable to believe that this property is a somewhat necessary feature of good absorbers; however, and quite counterintuitively, we show in the following that it is in principle possible to design a scatterer that absorbs as much power as desired, without any minimum bound on its scattering level. In a related context, it has been recently shown that cloaking layers may be able to arbitrarily decrease the total scattering from a receiving sensor [13–19] and efficiently form minimum-scattering designs. However, while the ratio of absorbed over scattered power may be unbounded, also here a fundamental trade-off appears between total available absorption and the amount of achievable scattering reduction [18]. To overcome this issue, arrays of impedance-matched receivers have been proposed to minimize reflection, or scattering in specific directions, while being able to retain an optimal absorption level by increasing the scattering towards other directions [20]. It appears that all these solutions are fundamentally limited to a trade-off between maximum achievable absorption and minimum-scattering signature when integrated over all angles.

In order to devise a way to overcome these limitations, in the following we discuss the possibility of staggering multiple absorption channels in a single receiver in order to increase the overall absorption efficiency η_{abs}, defined as the ratio between absorbed and scattered power, while not sacrificing the accessible amount of absorption. Our theory envisions the possibility of realizing *superabsorbing minimum-scattering sensors*, applicable to a broad range of frequencies, ranging from radio-frequency receiving antennas to optical sensors and absorbers, with exciting possibilities in biomedical technology, security, energy harvesting, sensing, and imaging.

Assuming for simplicity a spherical scatterer, its Mie coefficients $C_n^{\text{TM,TE}}$, fully describing its scattering and absorption properties as a function of its geometry, may be written under an $e^{-i\omega t}$ time convention in the form

$$C_n^{\text{TM,TE}} = \left(-1 + i\zeta_n^{\text{TM,TE}}\right)^{-1}. \tag{1}$$

These coefficients relate the impinging transverse-electric (TE) and transverse-magnetic (TM) spherical harmonic amplitudes to the scattered ones, and expressions for the case of layered spheres may be found in closed form [21]. In the limit of no absorption, ζ_n is a real number, which determines the strength of the corresponding scattered spherical harmonic: For $\zeta_n = 0$, in particular, we hit the nth harmonic resonance in the lossless limit, which maximizes the associated scattering. In the presence of loss, it is easy to prove that $\zeta_{nR} = \text{Re}[\zeta_n]$ specifies the modal dispersion and reactive response, while $\zeta_{nI} = \text{Im}[\zeta_n] > 0$, for passive inclusions, is directly related to the level of absorption.

The total absorption cross section of the sphere is generally given by

$$\begin{aligned}\sigma_{\text{abs}} &= \frac{-\lambda_0^2}{2\pi}\left(\sum_{n=1}^{N}(2n+1)\left(\text{Re}\left[C_n^{\text{TM}}\right] + \left|C_n^{\text{TM}}\right|^2\right)\right.\\ &\quad\left. + \sum_{m=1}^{M}(2m+1)\left(\text{Re}\left[C_m^{\text{TE}}\right] + \left|C_m^{\text{TE}}\right|^2\right)\right)\\ &= \sum_{n=1}^{N}\sigma_{\text{abs},n}^{\text{TM}} + \sum_{m=1}^{M}\sigma_{\text{abs},m}^{\text{TE}},\end{aligned} \tag{2}$$

in which we assumed that only the first N TM and M TE harmonics are of practical relevance, since the summations over all harmonics are convergent series.

The partial absorption cross section associated with each harmonic reaches its maximum $\sigma_{\text{abs},n}^{\max} = (2n+1)\,\lambda_0^2/8\pi$ under the condition $\zeta_{nR} = 0$, $\zeta_{nI} = 1$, which corresponds to ideal conjugate matching, i.e., to the case in which the reactive energy is balanced (resonance) and the radiation and absorption resistances are equal. Conventional antennas [22] are typically tuned to hit this condition, at the price of producing a scattering cross section equal to the absorption cross section, $\sigma_{\text{sca}} = \sigma_{\text{abs}}|_{\zeta_{nR}=0,\ \zeta_{nI}=1}$ [6], as illustrated in the inset of Fig. 1, showing the variation of absorption and scattering as a function of the amount of loss (ζ_{nI}) in a scatterer at resonance $\zeta_{nR} = 0$.

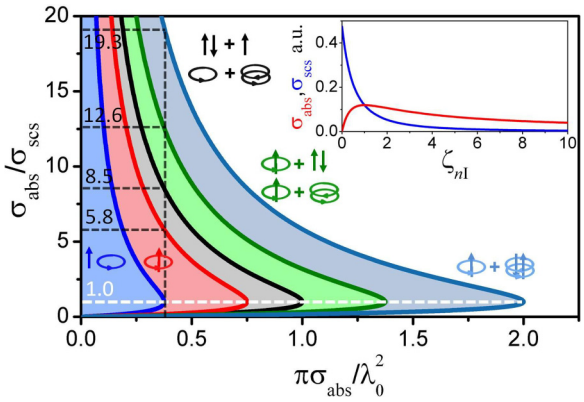

FIG. 1. (Color online) Absorption efficiency vs normalized absorbed cross section for an arbitrary passive receiver, considering TM_1 or TE_1 (blue region), TM_1 and TE_1 (red region), TM_1 and TM_2 or TE_1 and TE_2 (black region), $TM_{1,2}$ and TE_1 or $TE_{1,2}$ and TM_1 (green region), and $TM_{1,2}$ and $TE_{1,2}$ (dark blue region) spherical harmonics to contribute to the total scattering signature. Solid lines limiting each region correspond to the balanced resonance condition (3). Conjugate-matched points, corresponding to maximum absorption, all lie along $\eta_{abs} = 1$ (dashed white line) and the black dashed lines indicate the achievable values of absorption efficiency for a given level of absorbed power. A typical absorption/scattering cross-section diagram is shown in the inset as a function of the level of loss ζ_{nI} for a resonant harmonic $\zeta_{nR} = 0$.

As expected, at the crossing between red (σ_{abs}) and blue (σ_{sca}) lines, absorption is maximized.

Passivity ($\zeta_{nI} > 0$) poses inherent restrictions on the allowed values of total absorption efficiency $\eta_{abs} = \sigma_{abs}/\sigma_{sca}$ achievable for a given level of total absorption. This is shown in Fig. 1, which plots the absorption efficiency versus normalized absorption cross section for various receiving systems. The blue shaded region refers to the common situation in which the scattering is dominated by only one dipolar ($n = 1$) harmonic, either electric or magnetic, which is usually the case for small absorbers and receivers. The plot confirms that it is not possible in this scenario to absorb more than $\sigma_{abs,1}^{max}$, which corresponds to the rightmost point of the blue shadowed region, for which $\eta_{abs} = 1$ (conjugate-matched absorber). For lower levels of absorption, η_{abs} is necessarily bounded between a maximum and minimum value, as indicated by the solid blue line ($\zeta_{1R} = 0$), and a value of $\eta_{abs} > 1$ may only be achieved through trading off some absorption [18].

A way to overcome these inherent limitations is to consider the possibility of exciting more than one harmonic at the same time. For instance, the limit on maximum possible absorption may be overcome by staggering a few resonant harmonics, realizing a superabsorber [23], which is in some sense analogous to the superscatterer concept originally introduced in Ref. [24]. These higher-order scattering harmonics may be excited by increasing the electrical size of the object [25]. The different shaded regions in Fig. 1 correspond to different combinations of consecutive scattering orders for $n,m = 1,2$: The red region corresponds to the combination of electric and magnetic dipolar scattering, the black region to the combination of one dipolar and one quadrupolar mode, the green region to two dipolar and one quadrupolar, and finally the dark blue region to the combination of two dipolar and two quadrupolar modes, as indicated by the symbols in the figure. It is seen that, as we consider the contributions of different scattering harmonics, it is possible to push the maximum available σ_{abs} to larger values, where the maximum absorption for spherical scatterers is generally given by $\sigma_{abs}^{max} = (N^2 + 2N + M^2 + 2M)\frac{\lambda_0^2}{8\pi}$.

Also in this case, unitary absorption efficiency (white dashed line) is obtained at these maxima, when all scattering harmonics are independently conjugate matched. Operating such a superabsorbing system, however, is challenging in practice, especially when considering nanoparticles, because the Q factor and corresponding inverse bandwidth of a subwavelength resonant system grows very fast with n for fixed volume, and therefore the available bandwidth and sensitivity of such designs would be inherently limited [25,26]. This explains why practical realizations of small sensors and absorbers are typically limited to one or two resonant dipolar modes and do not involve higher-order resonances.

Figure 1, however, provides useful insights into the possibility of staggering various harmonics in order to minimize the scattering, while keeping the absorption at a desired large level α_{abs}. Imagine, for instance, that our goal is to absorb $\alpha_{abs} = \sigma_{abs,1}^{max} = 3\lambda_0^2/(8\pi)$, i.e., the maximum absorption available with one dipolar harmonic (vertical dashed line in Fig. 1). The figure indicates that, by staggering a few harmonics, we can attain in principle any arbitrary value of absorption efficiency, without sacrificing absorption. For example, by operating with one dipolar and one quadrupolar order (black shadowed region), we may be able to achieve an absorption efficiency as high as 8.55 while absorbing α_{abs}. Two dipolar and two quadrupolar modes (cyan region) may achieve a scattering almost 20 times lower than the absorption, for the same α_{abs}. For a given level of absorption, it is found that scattering is minimized if and only if

$$\zeta_{nR}^{TM} = \zeta_{mR}^{TE} = 0, \quad \zeta_{nI}^{TM} = \zeta_{mI}^{TE} = \frac{-4\pi\alpha_{abs} + [N(N+2) + M(M+2)]\left(1 + \sqrt{1 - \frac{8\pi\alpha_{abs}}{\lambda_0^2[N(N+2)+M(M+2)]}}\right)\lambda_0^2}{4\pi\alpha_{abs}} = \zeta_{opt}^{M,N}. \quad (3)$$

Interestingly, substituting these values into the expressions for scattering and absorption cross sections, we find that the corresponding maximum absorption efficiency has the identical value, $\eta_{max} = \zeta_{opt}^{M,N}$.

Equation (3) shows, as expected, that for $\alpha_{abs} = \sigma_{abs}^{max}$ we get $\eta_{max} = 1$, which is obtained when all coefficients are conjugate matched, i.e., all $\xi_n = i$. For smaller α_{abs}, however, still equal or larger than $3\lambda_0^2/(8\pi)$, large absorption efficiencies are accessible. To achieve maximum efficiency, according to condition (3) each harmonic has to be at resonance $\zeta_{nR}^{TE,TM} = 0$, but they should be all largely mismatched at the same level $\zeta_{nI}^{TE,TM} \gg 1$. All contributing harmonics, under this

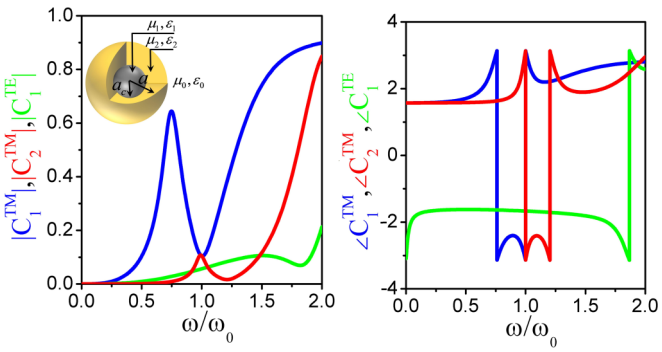

FIG. 2. (Color online) Amplitude and phase spectra of the first three scattering harmonics for the proposed superabsorber. The core-shell nanoparticle consists of a nonmagnetic dielectric core with permittivity $\varepsilon_1/\varepsilon_0 = 3.5 + i0.3$ and radius $a_c = 0.126\lambda_0$, and a plasmonic gold shell with outer radius $a = 0.15\lambda_0$, designed to operate at $\lambda_0 = 500$ nm. A schematic plot of the core-shell nanoparticle is shown in the inset.

condition, provide an amount of absorption proportional to their order, proving that the optimal strategy is to combine various mismatched harmonics, all balanced together to realize an optimal superabsorber with minimized visibility. Even more remarkably, in this scenario, the excitation of higher-order harmonics does not introduce relevant constraints on the bandwidth of operation, since each mode is largely mismatched, lowering the Q factor and sensitivity, and broadening the overall bandwidth.

This result is perfectly consistent with the optical or forward-scattering theorem [27]: Large absorption is directly associated to a proportional amount of real-valued scattered fields in the forward direction (a far-field shadow behind the object produced by a polarization current in phase with the impinging field) [28] and all other residual scattering does not directly impact power conservation. For this reason, a directive scattering pattern in phase with the impinging field and pointing towards the forward direction is ideal to minimize the overall scattering of the object [4], and this may be only realized by relying on higher-order scattering harmonics. There is in principle no limit on absorption efficiency, *independent of the level of desired absorption*, as long as we can rely on the suitable excitation of higher-order scattering harmonics to generate this directive pattern. Equation (3) determines the optimal excitation based on the suitable interference of $N + M$ spherical orders.

To provide further insights into this finding, we propose in the following a few examples of minimum-scattering superabsorbers in the form of layered nanospheres, as schematically shown in the inset of Fig. 2. We optimize the geometry of all our absorbers to operate at the operating wavelength $\lambda_0 = 500$ nm [29]. In our first example, the structure consists of a low-loss dielectric core with permittivity $\varepsilon_1/\varepsilon_0 = 3.5 + i0.3$ and a concentric shell made of a plasmonic metal, i.e., gold, modeled with Drude permittivity $\varepsilon_p/\varepsilon_0 = \varepsilon_\infty - \frac{\omega_p^2}{\omega(\omega+i\Gamma)}$ with $\varepsilon_\infty = 1.53$, $\omega_p = 2\pi$ 2069 THz, and $\Gamma = 2\pi$ 17.64 THz [30]. We fix the outer radius of the nanoparticle to be subwavelength, $a = 0.15\lambda_0$ (second row in Table I), and explore the possibility of simultaneously exciting the first two electric harmonics TM_1 and TM_2, corresponding to the shaded black region in Fig. 1. We set our desired absorption level to the maximum achievable with a single dipolar resonance $\alpha_{abs} = \frac{3\lambda_0^2}{8\pi}$ (the black dashed line in Fig. 1), and tune the ratio $a_c/a = 0.83$ to satisfy conditions (3).

The spectral dependence of the first three scattering coefficients for this optimized superabsorber is shown in Fig. 2. Around the central frequency, both the amplitude and phase of the TM_1 and TM_2 coefficients match each other: $\zeta_{1R}^{TM} \approx \zeta_{2R}^{TM} \approx 0$, $\zeta_{1I}^{TM} \approx \zeta_{2I}^{TM} \approx 8.51$, in excellent agreement with condition (3). The corresponding scattering coefficients become purely real, with the value $C_1^{TM} = C_2^{TM} = -0.105$, guaranteeing the most directive scattering pattern in the forward direction that can be supported by the interference of these two harmonics and suppressing the unwanted out-of-phase component of the scattering. As seen in the plots, in this regime, the next scattering coefficient, TE_1, is negligible.

By increasing the number of layers, it is possible to further increase the available degrees of freedom in our design, and study the evolution of this response as a function of the number of involved scattering orders. Figures 3(a)–3(c) show the scattering and absorption efficiencies versus frequency of different nanoparticles optimized to meet conditions (3) for two harmonics [TM_1 and TE_1, Fig. 3(a), $TM_{1,2}$, Fig. 3(b), consistent with Fig. 2], and three harmonics [$TM_{1,2}$ and TE_1, Fig. 3(c)], with design parameters summarized in Table I, respectively, first to third row. In each panel we also show for comparison the maximum absorption attainable from a conventional dipolar absorber with the same size (dashed red line), and the frequency dispersion of the calculated absorption efficiency (green dashed-dotted line). In the insets, we also show the scattering pattern from each particle in the E plane at the central frequency, showing a progressively more directive response as the number of modes and corresponding η_{abs} are increased.

We note various interesting features in these plots: First, despite the subwavelength features of all these designs,

TABLE I. Design parameters and performance characteristics of the proposed superabsorber designs.

Contributing harmonics	Number of layers	Radii	Permittivities	Peak absorption efficiency	Efficiency Q-factor
TM_1 and TE_1	3	$\{a_{c1},a_{c2},a\} = \{0.13,0.16,0.194\}\lambda_0$	$\varepsilon_1/\varepsilon_0 = 1.29 + i0.01$ ε_2 : Ag, $\varepsilon_3/\varepsilon_0 = 8.4 + i2.33$	7.1	6.9
TM_1 and TM_2	2	$\{a_c,a\} = \{0.126,0.15\}\lambda_0$	$\varepsilon_1/\varepsilon_0 = 3.5 + i0.3$, ε_2 : Au	7.9	10.4
$TM_{1,2}$ and TE_1	3	$\{a_{c1},a_{c2},a\} = \{0.25,0.28,0.31\}\lambda_0$	$\varepsilon_1/\varepsilon_0 = 1.25 + i0.03$ ε_2 : Ag, $\varepsilon_3/\varepsilon_0 = 8.6 + i0.96$	13.5	17

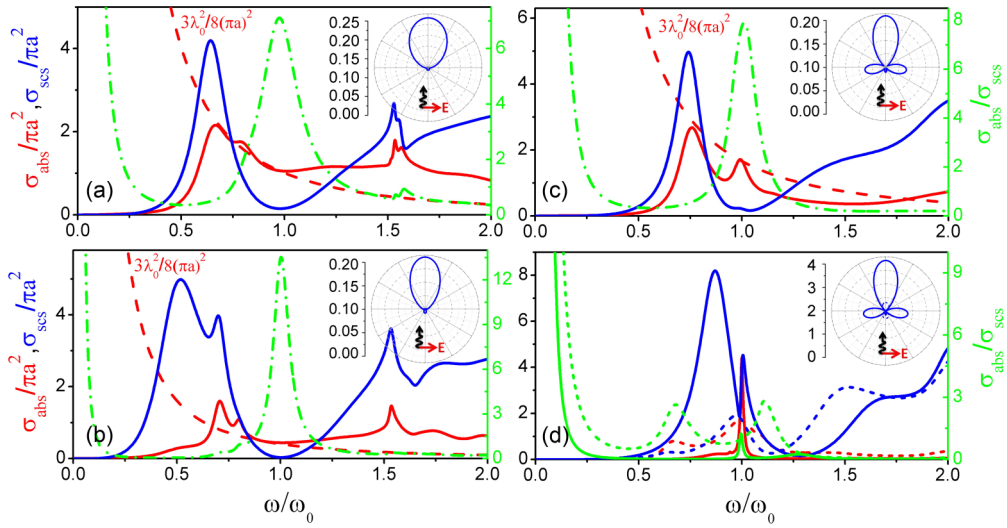

FIG. 3. (Color online) (a)–(c) Absorption (red line) and scattering (blue line) cross sections of optimal minimum-scattering superabsorbers relying on (a) TM_1 and TE_1, (b) $TM_{1,2}$, and (c) $TM_{1,2}$ and TE_1 harmonics, consistent with the geometries in Table I. The absorption cross section of a conjugate-matched dipole is also plotted for comparison in each panel (red dashed line). The E-plane scattering pattern is shown in each inset at the central frequency ω_0. The absorption efficiency of the sensor is shown in each panel by green lines. (d) Absorption (red) and scattering (blue) cross sections of conjugate-matched absorbers with one (dashed lines) and two (solid lines) harmonics and outer radius $a = 0.15\lambda_0$.

higher-order resonances can be excited quite straightforwardly with realistic parameters and materials since each harmonic is deeply mismatched by an intentionally large level of absorption resistance, bringing down the Q factor of each resonance. In particular, $|C_n| = 0.146, 0.105, 0.07$ for the three examples in Figs. 3(a)–3(c), respectively, significantly far from the conjugate-matched condition $|C_n| = 1/2$. This implies that the bandwidth is not significantly worsened, even after increasing the number of harmonics and their resonant order. To highlight this point, we calculated an effective Q factor (inverse fractional bandwidth) for the dispersion of the absorption efficiency, reported in the last column of Table I, indicating that the Q factor grows linearly with the absorption efficiency, remaining manageable even if a few higher-order harmonics are involved and the nanoparticle is still deeply subwavelength.

This property is in stark contrast with the example in Fig. 3(d), which shows for comparison the case of conjugate-matched resonant nanoparticles with the same size as the superabsorber of Fig. 3(b), but now designed to support dipolar (dashed lines) or combined $TM_{1,2}$ conjugate-matched resonances. It is found that in this case the Q factor drastically increases from 7 to 100, moving from one to two harmonics, while the absorption is increased by only a factor of 3. Our optimized minimum-scattering superabsorbers show the same absorption as an ideally conjugate-matched resonant dipole, or a coherent perfect absorbing dipole, while scattering 7–13 times less over a reasonable bandwidth and with realistic materials and robustness to imperfections in realization. The robustness of our design is studied in more detail in Ref. [31], where we demonstrate robust performance against variations in the values of the permittivity of the selected materials. Some of the material parameters of the dielectric layers considered in the previous examples may not be directly available at the frequency of interest. While variations around these optimal values do not significantly affect the overall performance [31], we stress that significantly more flexibility in the choice of materials may be attained by adding degrees of freedom to the geometry, such as considering asymmetric shapes, or compact clusters of nanoparticles [32]. In this case, it may be possible to realize the optimal condition (3) with a wide variety of available materials. In fact, suitably chosen asymmetric geometries may allow coupling different scattering channels together [32], further boosting the described effect.

It is also worth emphasizing that this is not simply the result of scattering cancellation, but it requires the careful excitation of various resonant modes in a balanced multimodal absorber. This is further outlined in Ref. [31], where near-field and far-field patterns are shown in detail for the minimum-scattering superabsorber of Figs. 2 and 3(b) in comparison to a conventional layered nanoparticle.

The balanced resonant design and minimum-scattering superabsorbing response described here may have exciting applications, including subdiffractive near-field imaging [1,2] and optimal absorbers with minimal impact on the impinging field distribution. We have shown in fact that, with a proper design, both absorption and absorption efficiency can be made arbitrarily large over a moderate yet reasonable bandwidth. These findings may also relax the constraints on the absorption of minimum-scattering antennas, providing an exciting venue to minimize the mutual coupling between closely packed receiving antennas. Probably the most striking feature of this concept resides in the moderate values of the Q factor associated with it, making the proposed designs realistic and quite robust to fabrication tolerances.

This work has been partially supported by AFOSR with the YIP Award No. FA9550-11-1-0009 and by the ONR MURI Grant No. N00014-10-1-0942.

[1] D. W. Pohl, W. Denk, and M. Lanz, Appl. Phys. Lett. **44**, 651 (1984).
[2] B. Hecht, B. Sick, U. P. Wild, V. Deckert, R. Zenobi, O. J. F. Martin, and D. W. Pohl, J. Chem. Phys. **112**, 7761 (2000).
[3] W. K. Kahn and H. Kurss, IEEE Trans. Antennas Propag. **13**, 671 (1965).
[4] J. B. Andersen and A. Frandsen, IEEE Trans. Antennas Propag. **53**, 2843 (2005).
[5] M. Gustafsson, C. Sohl, and G. Kristensson, Proc. R. Soc. A **463**, 2589 (2007).
[6] D. H. Kwon and D. M. Pozar, IEEE Trans. Antennas Propag. **57**, 3720 (2009).
[7] A. Kurs, A. Karalis, R. Moffatt, J. D. Joannopoulos, P. Fisher, and M. Soljacic, Science **317**, 83 (2007).
[8] J. Lee and S. Nam, IEEE Trans. Antennas Propag. **58**, 3442 (2010).
[9] D. M. Pozar, *Microwave Engineering* (Wiley, New York, 1997).
[10] Y. D. Chong, L. Ge, H. Cao, and A. D. Stone, Phys. Rev. Lett. **105**, 053901 (2010).
[11] R. Green, IEEE Trans. Antennas Propag. **14**, 17 (1966).
[12] A. Alu and S. Maslovski, IEEE Trans. Antennas Propag. **58**, 1436 (2010).
[13] A. Alù and N. Engheta, Phys. Rev. Lett. **102**, 233901 (2009).
[14] G. Castaldi, I. Gallina, V. Galdi, A. Alù, and N. Engheta, J. Opt. Soc. Am. B **27**, 2132 (2010).
[15] A. Greenleaf, Y. Kurylev, M. Lassas, and G. Uhlmann, Phys. Rev. E **83**, 016603 (2011).
[16] A. Alù and N. Engheta, Phys. Rev. Lett. **105**, 263906 (2010).
[17] P. Y. Fan, U. K. Chettiar, L. Y. Cao, F. Afshinmanesh, N. Engheta, and M. L. Brongersma, Nat. Photonics **6**, 380 (2012).
[18] R. Fleury, J. Soric, and A. Alù, Phys. Rev. B **89**, 045122 (2014).
[19] A. Alù and N. Engheta, Phys. Rev. E **72**, 016623 (2005).
[20] A. Karilainen and S. Tretyakov, IEEE Trans. Antennas Propag. **60**, 3471 (2012).
[21] A. Alù and N. Engheta, J. Appl. Phys. **97**, 094310 (2005).
[22] C. A. Balanis, *Antenna Theory* (Wiley, New York, 1996).
[23] S. A. Mann and E. C. Garnett, Nano Lett. **13**, 3173 (2013).
[24] Z. Ruan and S. Fan, Phys. Rev. Lett. **105**, 013901 (2010).
[25] C. F. Bohren and D. R. Huffman, *Absorption and Scattering of Light by Small Particles* (Wiley, New York, 1983).
[26] A. Alù and N. Engheta, IEEE Trans. Antennas Propag. **55**, 3027 (2007).
[27] A. Ishimaru, *Wave Propagation and Scattering in Random Media* (Academic, New York, 1978).
[28] A. Alu and N. Engheta, J. Nanophotonics **4**, 041590 (2010).
[29] We stress that this choice of operating frequency is completely arbitrary: The proposed concept is applicable to different classes of sensors and absorbers, ranging from simple loaded wire antennas at radio frequencies to nanoparticle sensors and absorbers at optical frequencies.
[30] M. A. Ordal, R. J. Bell, R. W. Alexander, Jr., L. L. Long, and M. R. Querry, Appl. Opt. **24**, 4493 (1985).
[31] See Supplemental Material at http://link.aps.org/supplemental/10.1103/PhysRevB.89.121416 for further details on the optical response of minimum-scattering superabsorbers, as well as their robustness to perturbations of the design parameters.
[32] F. Shafiei, F. Monticone, K. Q. Le, X. X. Liu, T. Hartsfield, A. Alù, and X. Li, Nat. Nanotechnol. **8**, 95 (2013).